Journal of Sound and Vibration (2000) **230**(1), 1–29
doi:10.1006/jsvi.1999.2601, available online at http://www.idealibrary.com on IDEAL®

INFLUENCE OF PERMANENT TURBULENT AIR FLOW ON ACOUSTIC STREAMING

L.-C. VALDÈS AND D. SANTENS

Groupe de Recherche Energies et Environnement, Université de Valenciennes et du Hainaut-Cambrésis, France

(*Received* 14 *December* 1998, *and in final form* 14 *June* 1999)

Permanent turbulent air flow at low Mach number does not disturb the longitudinal gradient of mean pressure associated with acoustic streaming, while the profile of mean axial velocities of the air flow is not appreciably modified when it is subjected to the wave generating the acoustic streaming. This is highlighted by the present experiments and discussed in the theoretical framework initially proposed by Rayleigh, then generalized by Nyborg and Westervelt. The result is, on the one hand, the possibility of predicting simply the Reynolds stress exerted on a permanent turbulent air flow subjected to a wave generating acoustic streaming, and on the other hand, the very likely absence of any influence of permanent turbulent air flow on acoustic streaming.

1. INTRODUCTION

Acoustic fields emitted into propagation mediums at rest can generate significant mean flows, referred to as acoustic streaming. Initial observation of this phenomenon can be traced back to Faraday [1]. Rayleigh [2] provided a satisfactory interpretation based on the concepts stressed by Reynolds [3] on turbulence. Acoustic velocities, having a role similar to that of turbulent velocity fluctuations within turbulent flows, are at the origin of stress acting specifically on the mean pressure and velocities fields of the flow. Nyborg [4] and Westervelt [5] completed this interpretation in broadening the basic hypotheses of Rayleigh's theoretical framework. Lighthill's paper [6] and book [7] bring together current knowledge on this subject.

During the 1980s, researchers showed great interest in the phenomenon of interaction between flows and forced acoustic fields. One potential use could be that of flows being driven by acoustic fields. To paint an overall picture of the preoccupations that concerned them, the following may be cited: Ahuja *et al.* [8] Blevins [9], Davis and Strahle [10], Ffowcs-Williams [11], Lowson [12], or Shearin and Jones [13]. The theoretical framework of these authors is that of the theory of wave instability, which Tam [14] for example, applies convincingly to the interaction between acoustic waves and flows.

0022-460X/00/060001 + 29 $35.00/0

A natural question arising from the study on acoustic streaming in mediums at rest is to determine what it becomes when acoustic waves are emitted into flowing mediums. According to the considerations of the authors cited above, the solution to this question, which comes under the phenomenon of interaction between acoustic fields and flows, is to be found in the context of the wave instability theory. However, the theoretical framework of acoustic streaming should not be put aside *a priori*. Indeed, by using the latter theory to interpret the phenomenon of the separation of hot and cold air fluxes observed in the vortex-tube [15, 16], Kurosaka [17] demonstrated that the theoretical framework of acoustic streaming could be employed outside the field of application initially envisaged by Rayleigh [2], and later, Nyborg [4] and Westervelt [5]: the field of propagation mediums initially at rest.

The interest here is the eventual modifications that forced flows cause on the acoustic streaming. The geometry considered is that of a tube and the situation is simplified to forced permanent turbulent axial flows, at low Mach number. The acoustic fields are generated by the emission of monochromatic plane waves. Section 2 establishes formulas describing permanent turbulent air flow, acoustic streaming generated by acoustic waves emitted in air at rest and the said air flow subjected to the said waves. The general modelling, which is that of statistical equations of fluid mechanics, allows Reynolds stress as a characteristic quantity. The experimental study presented in section 3 provides empirical data which can be interpreted in terms of Reynolds stress. On the basis of data presented in section 3, the validity of the modelling in section 2 is examined (section 4) and that of the theoretical framework of statistical equations of fluid mechanics is then shown. The more significant experimental results are interpreted in section 5; a simple analytical relation between the Reynolds stresses relative to the air flow, the acoustic streaming and the air flow subjected to the wave generating the acoustic streaming is deduced and it is shown that permanent turbulent air flow has very likely no influence on acoustic streaming.

2. THEORETICAL MODELLING

The present section recalls the standard theoretical framework for stationary turbulent air flows and acoustic streaming. Only the results relative to acoustic streaming in turbulent flowing mediums that do not require any peculiar hypothesis are presented here.

2.1. GENERAL EQUATIONS OF CYLINDRICAL TURBULENT INCOMPRESSIBLE FLOW OF STATIONARY STATISTIC MEAN

The systems considered are composed of air at room temperature, flowing in cylindrical tubes at low velocities compared with the speed of sound (low Mach number). It is well known that such flows are described by mass balance and momentum balance equations relative to incompressible fluids. In a system of cylindrical co-ordinates fixed to the tube, the flow variables which form the volumic

mass ρ, static pressure p, and the velocity co-ordinates (v_r, v_θ, v_z) verify the following general relationships (see for example, reference [18]):

$$\partial_r v_r + \frac{\partial_\theta v_\theta}{r} + \partial_z v_z + \frac{v_r}{r} = 0 \tag{1}$$

and

$$\partial_t v_r + v_r \partial_r v_r + v_\theta \frac{\partial_\theta v_r}{r} + v_z \partial_z v_r - \frac{v_\theta^2}{r} = -\frac{1}{\rho}\partial_r p + \nu \left[\partial^2_{r^2} v_r + \frac{\partial^2_{\theta^2} v_r}{r^2} + \partial^2_{z^2} v_r + \frac{\partial_r v_r}{r} - 2\frac{\partial_\theta v_\theta}{r^2} - \frac{v_r}{r^2} \right],$$

$$\partial_t v_\theta + v_r \partial_r v_\theta + v_\theta \frac{\partial_\theta v_\theta}{r} + v_z \partial_z v_\theta + \frac{v_r v_\theta}{r} = -\frac{1}{\rho}\frac{\partial_\theta p}{r} + \nu \left[\partial^2_{r^2} v_\theta + \frac{\partial^2_{\theta^2} v_\theta}{r^2} + \partial^2_{z^2} v_\theta + \frac{\partial_r v_\theta}{r} + 2\frac{\partial_\theta v_r}{r^2} - \frac{v_\theta}{r^2} \right],$$

$$\partial_t v_z + v_r \partial_r v_z + v_\theta \frac{\partial_\theta v_z}{r} + v_z \partial_z v_z = -\frac{1}{\rho}\partial_z p + \nu \left[\partial^2_{r^2} v_z + \frac{\partial^2_{\theta^2} v_z}{r^2} + \partial^2_{z^2} v_z + \frac{\partial_r v_z}{r} \right]. \tag{2}$$

The air being at a uniform and constant temperature, the kinematic viscosity of air, ν is constant.

In the air flows considered, the velocity and pressure fluctuations occur either due to the turbulence, or due to the acoustic vibrations. To describe them, it is standard to write out the linearization in equations (1) and (2):

$$p = \bar{p} + p', \qquad v_r = \bar{v}_r + v'_r,$$
$$v_\theta = \bar{v}_\theta + v'_\theta, \qquad v_z = \bar{v}_z + v'_z, \tag{3}$$

where the overlined values indicate the mean statistic and the apostrophe, the fluctuation.

In practise, the mean determined most simply is the temporal one. In the case of flows whose means are stationary, it is generally admitted that, as a result of the frequently evoked ergodicity hypothesis, the statistical and temporal means of the variables coincide. Subsequently, it is supposed that the mean values of the turbulent flows studied are stationary. Moreover, with this hypothesis, the partial derivatives of means in relation to time are zero.

Writing out the linearizations (3) in equations (1) and (2), by taking the mean of the two elements in the equations and applying the nil properties of the fluctuation mean and commutation of the mean and the derivation, equations (1) and (2) become

$$\partial_r \bar{v}_r + \frac{\partial_\theta \bar{v}_\theta}{r} + \partial_z \bar{v}_z + \frac{\bar{v}_r}{r} = 0, \tag{4}$$

$$\bar{v}_r\partial_r\bar{v}_r + \bar{v}_\theta\frac{\partial_\theta\bar{v}_r}{r} + \bar{v}_z\partial_z\bar{v}_r - \frac{\bar{v}_\theta^2}{r} = -\frac{1}{\rho}\partial_r\bar{p} + \nu\left[\partial^2_{r^2}\bar{v}_r + \frac{\partial^2_{\theta^2}\bar{v}_r}{r^2} + \partial^2_{z^2}\bar{v}_r + \frac{\partial_r\bar{v}_r}{r} - 2\frac{\partial_\theta\bar{v}_\theta}{r^2} - \frac{\bar{v}_r}{r^2}\right] - \bar{\tau}_r,$$

$$\bar{v}_r\partial_r\bar{v}_\theta + \bar{v}_\theta\frac{\partial_\theta\bar{v}_\theta}{r} + \bar{v}_z\partial_z\bar{v}_\theta + \frac{\bar{v}_r\bar{v}_\theta}{r} = -\frac{1}{\rho}\frac{\partial_\theta\bar{p}}{r} + \nu\left[\partial^2_{r^2}\bar{v}_\theta + \frac{\partial^2_{\theta^2}\bar{v}_\theta}{r^2} + \partial^2_{z^2}\bar{v}_\theta + \frac{\partial_r\bar{v}_\theta}{r} + 2\frac{\partial_\theta\bar{v}_r}{r^2} - \frac{\bar{v}_\theta}{r^2}\right] - \bar{\tau}_\theta,$$

$$\bar{v}_r\partial_r\bar{v}_z + \bar{v}_\theta\frac{\partial_\theta\bar{v}_z}{r} + \bar{v}_z\partial_z\bar{v}_z = -\frac{1}{\rho}\partial_z\bar{p} + \nu\left[\partial^2_{r^2}\bar{v}_z + \frac{\partial^2_{\theta^2}\bar{v}_z}{r^2} + \partial^2_{z^2}\bar{v}_z + \frac{\partial_r\bar{v}_z}{r}\right] - \bar{\tau}_z. \quad (5)$$

Equations (4) and (5) appear in a mathematical form similar to that of equations (1) and (2). The terms $\bar{\tau}_r$, $\bar{\tau}_\theta$ and $\bar{\tau}_z$, which are not found in the latter, come from the mean of the squares or the cross-products of velocity fluctuations. Thus they are expressed as

$$\bar{\tau}_r = \overline{v_r'\partial_r v_r'} + \overline{v_\theta'\frac{\partial_\theta v_r'}{r}} + \overline{v_z'\partial_z v_r'} - \frac{\overline{v_\theta'^2}}{r},$$

$$\bar{\tau}_\theta = \overline{v_r'\partial_r v_\theta'} + \overline{v_\theta'\frac{\partial_\theta v_\theta'}{r}} + \overline{v_z'\partial_z v_\theta'} + \frac{\overline{v_r'v_\theta'}}{r},$$

$$\bar{\tau}_z = \overline{v_r'\partial_r v_z'} + \overline{v_\theta'\frac{\partial_\theta v_z'}{r}} + \overline{v_z'\partial_z v_z'}. \quad (6)$$

They are referred to as components of Reynolds stress $\bar{\boldsymbol{\tau}}$. The latter is interpreted as stress produced within the fluid by velocity fluctuations. Their particularity is to exert on the mean flow.

2.2. MODELLING PERMANENT TURBULENT FLOW SUBJECTED TO THE WAVES GENERATING ACOUSTIC STREAMING

The purpose of the hypotheses that authors have made, in particular Rayleigh [2], then Nyborg [4] and Westervelt [5], is to cancel the non-linear terms in the left-hand side of equations (5). This enables the analytical solutions for acoustic streaming. However, cancelling the convective derivatives renders the description of acoustic streaming in air flows inadequate. For this reason, equations (4) and (5) with all terms have been adopted as the basis of the description of the mean air flow in a tube, subjected to velocity and pressure fluctuations.

Subsequently, three configurations of the system will be considered: (1) a turbulent air flow, forced by suction to a tube end, (2) propagation of an acoustic wave emitted through a tube end into the air initially at rest, (3) propagation of the wave in the turbulent air flow. Equations governing the system studied in each of these three configurations will be established in sufficiently

normal and simple conditions so that they are written out easily for calculation and experimental verification.

In configuration (1), the turbulent air flow is, moreover, taken to be axial and permanent. This brings about axisymmetry and leads to assume that the mean scalar variables, noted here as $\bar{v}_{(1)r}$, $\bar{v}_{(1)\theta}$, $\bar{v}_{(1)z}$ and $\bar{p}_{(1)}$, verify, respectively, as

$$\partial_\theta \cdot < 0 \text{ with, in particular, } \bar{v}_{(1)\theta} = 0 \tag{7}$$

and

$$\bar{v}_{(1)r} = 0. \tag{8}$$

With relations at equations (7) and (8), the continuity at equation (4) becomes

$$\partial_z \bar{v}_{(1)z} = 0 \tag{9}$$

and the momentum balance equations (5) can be written

$$\begin{aligned}
\bar{\tau}_{(1)r} &= -\frac{1}{\rho}\partial_r \bar{p}_{(1)}, \\
\bar{\tau}_{(1)\theta} &= 0, \\
\bar{\tau}_{(1)z} &= -\frac{1}{\rho}\partial_z \bar{p}_{(1)} + \nu\left[\partial^2_{r^2}\bar{v}_{(1)z} + \frac{\partial_r \bar{v}_{(1)z}}{r}\right].
\end{aligned} \tag{10}$$

In configuration (2), the acoustic wave is assumed to be monochromatic, plane and axisymmetric. It is assumed to be attenuated in its propagation through the air at rest contained within the tube, so that this well-known critical condition for waves to generate acoustic streaming is realized. The mean scalar variables, noted in the present configuration as $\bar{v}_{(2)r}$, $\bar{v}_{(2)\theta}$, $\bar{v}_{(2)z}$ and $\bar{p}_{(2)}$, are then relative to acoustic streaming. As this is generated by axisymmetric waves in boundary conditions which have axisymmetry, the acoustic streaming also will have axisymmetry. This gives

$$\partial_\theta \cdot < 0 \tag{11}$$

with, in particular:

$$\bar{v}_{(2)\theta} = 0. \tag{12}$$

The mass balance equation (4) is written as

$$\frac{\partial_r(r\bar{v}_{(2)r})}{r} + \partial_z \bar{v}_{(2)z} = 0 \tag{13}$$

and the momentum balance equations (5) lead to

$$\begin{aligned}
\bar{\tau}_{(2)r} &= -\bar{v}_{(2)r}\partial_r \bar{v}_{(2)r} - \bar{v}_{(2)z}\partial_z \bar{v}_{(2)r} - \frac{1}{\rho}\partial_r \bar{p}_{(2)} + \nu\left[\partial^2_{r^2}\bar{v}_{(2)r} + \partial^2_{z^2}\bar{v}_{(2)r} + \frac{\partial_r \bar{v}_{(2)r}}{r} - \frac{\bar{v}_{(2)r}}{r^2}\right], \\
\bar{\tau}_{(2)\theta} &= 0, \\
\bar{\tau}_{(2)z} &= -\bar{v}_{(2)r}\partial_r \bar{v}_{(2)z} - \bar{v}_{(2)z}\partial_z \bar{v}_{(2)z} - \frac{1}{\rho}\partial_z \bar{p}_{(2)} + \nu\left[\partial^2_{r^2}\bar{v}_{(2)z} + \partial^2_{z^2}\bar{v}_{(2)z} + \frac{\partial_r \bar{v}_{(2)z}}{r}\right].
\end{aligned} \tag{14}$$

The considerations concerning the symmetry of the acoustic field still apply to configuration (3). The flow scalar variables being $\bar{v}_{(3)r}$, $\bar{v}_{(3)\theta}$, $\bar{v}_{(3)z}$ and $\bar{p}_{(3)}$, equations (4) and (5), respectively, lead to

$$\frac{\partial_r(r\bar{v}_{(3)r})}{r} + \partial_z \bar{v}_{(3)z} = 0 \tag{15}$$

and

$$\bar{\tau}_{(3)r} = -\bar{v}_{(3)r}\partial_r \bar{v}_{(3)r} - \bar{v}_{(3)z}\partial_z \bar{v}_{(3)r} - \frac{1}{\rho}\partial_r \bar{p}_{(3)} + \nu\left[\partial^2_{r^2}\bar{v}_{(3)r} + \partial^2_{z^2}\bar{v}_{(3)r} + \frac{\partial_r \bar{v}_{(3)r}}{r} - \frac{\bar{v}_{(3)r}}{r^2}\right],$$

$$\bar{\tau}_{(3)\theta} = 0,$$

$$\bar{\tau}_{(3)z} = -\bar{v}_{(3)r}\partial_r \bar{v}_{(3)z} - \bar{v}_{(3)z}\partial_z \bar{v}_{(3)z} - \frac{1}{\rho}\partial_z \bar{p}_{(3)} + \nu\left[\partial^2_{r^2}\bar{v}_{(3)z} + \partial^2_{z^2}\bar{v}_{(3)z} + \frac{\partial_r \bar{v}_{(3)z}}{r}\right]. \tag{16}$$

In each of the three configurations, the components of Reynolds stresses $\bar{\boldsymbol{\tau}}_{(1)}$, $\bar{\boldsymbol{\tau}}_{(2)}$ and $\bar{\boldsymbol{\tau}}_{(3)}$ are expressed according to the velocity fluctuations via formulas at equation (6). The velocity fluctuations in configuration (1), essentially due to the turbulence, are purely random and predictable only statistically; the Reynolds stress, they are associated with, will be designed by turbulent stress. The velocity fluctuations in configuration (2) corresponding to acoustic vibrations are, on the contrary, purely periodic and may be calculated exactly; Reynolds stress, they are associated with, will be designed by acoustic stress. For their calculation, it is sufficient only to know the field of acoustic velocity.

2.3. ACOUSTIC STRESS IN MEDIUM AT REST

The present calculation aims to determine the Reynolds stress in configuration (2), which is purely acoustic stress. The acoustic velocity field is first calculated.

The sound source is placed at the end, of abscissa $z_s = 0$, of a tube with radius a. It functions on a permanent regime and emits an acoustic wave into the air at rest, towards the z positives. This wave is, by hypothesis, monochromatic of pulsation ω, with no azimuthal modes. Its propagation takes place, moreover, in the linear domain at the speed of sound, c being a constant.

The field of acoustic pressure within the tube, which identifies to the pressure fluctuation $p'_{(2)}$, can be written *a priori*:

$$p'_{(2)} = \mathrm{e}^{\mathrm{j}\omega t} G(r, z). \tag{17}$$

It satisfies Helmholtz equation expressed in the system of natural cylindrical co-ordinates fixed to the tube. This equation does not contain any azimuth terms and can be written as

$$\frac{\partial_r(r\partial_r G)}{r} + \partial^2_{z^2} G + K^2 G = 0, \tag{18}$$

where the constant $K = \omega/c$ is the total wave number. Equation (18) allows as a general solution:

$$G(r, z) = (A_1 \mathrm{e}^{-\mathrm{j}kz} + A_2 \mathrm{e}^{\mathrm{j}kz}) \mathrm{J}_0(k_T r), \tag{19}$$

where J_0 denotes Bessel function of the first kind of order 0. Constants A_1, A_2, k and k_T are complex and depend on the boundary conditions of the different tube walls.

According to the momentum balance equation, which here takes the form of Euler equation,

$$\rho \partial_t \mathbf{v}'_{(2)} + \nabla p'_{(2)} = \mathbf{0}, \tag{20}$$

the acoustic velocity is also harmonic, with pulsation ω:

$$\mathbf{v}'_{(2)} = \mathrm{e}^{\mathrm{j}\omega t} \mathbf{v}'_0(r, z). \tag{21}$$

Its expression according to the previous constants is deduced from equation (20) and from the expression of acoustic pressure $p'_{(2)}$, drawn from relationships (19) and (17). The components of the spatial factor of complex velocity $\mathbf{v}'_0(r, z)$ may then be calculated:

$$\begin{aligned} v'_{0r} &= -\mathrm{j} \frac{k_T}{K} \frac{1}{\rho c} (A_1 \mathrm{e}^{-\mathrm{j}kz} + A_2 \mathrm{e}^{\mathrm{j}kz}) \mathrm{J}_1(k_T r), \\ v'_{0\theta} &= 0, \\ v'_{0z} &= \frac{k}{K} \frac{1}{\rho c} (A_1 \mathrm{e}^{-\mathrm{j}kz} - A_2 \mathrm{e}^{\mathrm{j}kz}) \mathrm{J}_0(k_T r). \end{aligned} \tag{22}$$

J_1 denotes Bessel function of the first kind of order 1.

Determining k and k_T uses the specific impedance of the lateral inner wall, $Z_T = z_T \mathrm{e}^{\mathrm{j}\psi}$, defined as

$$Z_T = \left. \frac{p'_{(2)}}{v'_{(2)r}} \right|_{r=a}. \tag{23}$$

By substituting relation (19) and the first equation of system (22) in relation (23) and by making the calculation hypothesis

$$k_T a \ll 1, \tag{24}$$

the calculation leads to

$$\begin{aligned} k_T^2 &= \mathrm{j} \frac{\rho c}{Z_T} \frac{2K}{a}, \\ k^2 &= K^2 - \mathrm{j} \frac{\rho c}{Z_T} \frac{2K}{a}. \end{aligned} \tag{25}$$

Determining the constants A_1 and A_2 uses the boundary conditions imposed on the cross-sections forming the tube ends. At the end of abscissa L, situated opposite the source, the wave is subjected to a reflection of coefficient $G = g\mathrm{e}^{\mathrm{j}\varphi}$. On the cross-section of the end carrying the source, acoustic velocity has, at the tube axis, a value of V_0 imposed by the source and the reflected waves in the stationary regime.

The calculation of A_1 and A_2 leads to the expression of $p'_{(2)}$:

$$p'_{(2)} = \mathrm{e}^{\mathrm{j}\omega t}\,\rho c\, V_0 \frac{K}{k}\,\mathrm{J}_0(k_T r)\,F(z), \tag{26}$$

where the auxiliary function $F(z)$ is given by

$$F(z) = \frac{\mathrm{e}^{-\mathrm{j}kz} + G\mathrm{e}^{\mathrm{j}k(z-2L)}}{1 - G\mathrm{e}^{-2\mathrm{j}kL}}. \tag{27}$$

The mean square pressure $p'^2_{(2)RMS} = \frac{1}{2}\,\overline{p'_{(2)}p'^*_{(2)}}$ is then calculated at the variable point of abscissa z. This gives

$$p'^2_{(2)RMS} = \frac{1}{2}\left[\rho c V_0 \frac{K}{|k|}|\mathrm{J}_0(k_T r)|\right]^2 . |F(z)|^2. \tag{28}$$

The expression of $|F(z)|^2$, adopted in further applications in section 4:

$$|F(z)|^2 = \frac{\mathrm{e}^{2k_i z} + g^2\mathrm{e}^{2k_i(L-z)} + 2g\mathrm{e}^{2k_i L}\cos[2k_r(L-z) - \varphi]}{1 + g^2\,\mathrm{e}^{4k_i L} - 2g\mathrm{e}^{2k_i L}\cos[2k_r L - \varphi]}, \tag{29}$$

is obtained by writing $k = k_r + \mathrm{j}k_i$.

The components of acoustic velocity, which are obtained in writing out the expression of constants A_1 and A_2 in relation (22), are

$$\begin{aligned} v'_{(2)r} &= -\,\mathrm{j}V_0 \frac{k_T}{k}\mathrm{e}^{\mathrm{j}\omega t}\,\mathrm{J}_1(k_T r)F(z), \\ v'_{(2)\theta} &= 0, \\ v'_{(2)z} &= V_0\,\mathrm{e}^{\mathrm{j}\omega t}\mathrm{J}_0(k_T r)\,H(z). \end{aligned} \tag{30}$$

The auxiliary function $H(z)$ is given by

$$H(z) = \frac{\mathrm{e}^{-\mathrm{j}kz} - G\mathrm{e}^{\mathrm{j}k(z-2L)}}{1 - G\mathrm{e}^{-2\mathrm{j}kL}}. \tag{31}$$

Lastly, the calculation of acoustic stress is realized by writing out relations (30) in formulas (6). It is facilitated by the hypothesis contained in relation (24). Bessel functions J_0 and J_1 may then be assimilated to their series expansion of order 1.

Conserving the real part of velocities and applying formulas (6), gives:

$$\bar{\tau}_{(2)r} = \frac{1}{2}\frac{p'^2_{(2)RMS}}{\rho^2\omega^2}|k_T|^2\, r\left[\frac{|k_T|^2}{2} - \left|\frac{H(z)}{F(z)}\right|^2 |k|^2 \sin(\psi)\right],$$

$$\bar{\tau}_{(2)\theta} = 0,$$

$$\bar{\tau}_{(2)z} = -\frac{p'^2_{(2)RMS}}{\rho^2\omega^2}\frac{|H(z)|}{|F(z)|}|k|\left[\frac{|k_T|^4}{4} r^2 \sin(\varphi_F - \varphi_H - \varphi_z) + |k|^2 \sin(\varphi_H - \varphi_F - \varphi_z)\right], \tag{32}$$

where

$$\varphi_r = \mathrm{Arg}(k_T^2) = \frac{\pi}{2} - \psi,$$

$$\varphi_z = \mathrm{Arg}(k),$$

$$\varphi_F = \mathrm{Arg}(F(z)),$$

$$\varphi_H = \mathrm{Arg}(H(z)).$$

The expression of $|H(z)|^2$ adopted in further applications in section 4:

$$|H(z)|^2 = \frac{e^{2k_i z} + g^2 e^{2k_i(L-z)} - 2g\, e^{2k_i L}\cos[2k_r(L-z) - \varphi]}{1 + g^2 e^{4k_i L} - 2g e^{2k_i L}\cos[2k_r L - \varphi]} \tag{33}$$

is obtained by writing $k = k_r + \mathrm{j}k_i$.

2.4. QUESTIONS RAISED BY MODELLING OF THE VELOCITY FLUCTUATIONS IN CONFIGURATION (3)

From the linearized equations of fluid mechanics, Kovasznay [19] showed that small fluctuations occur according to three modes: acoustic, entropic and rotational, connected with the particular type of propagation equation they verify. According to this theory, the velocity fluctuations $\mathbf{v}'_{(3)}$ that occur in configuration (3) are of the rotational type, written as $\mathbf{v}''_{(3)}$, and of the acoustic type, written as $\mathbf{v}^{\wedge}_{(3)}$. By hypothesis, they verify the linear relation of linear superposing:

$$\mathbf{v}'_{(3)} = \mathbf{v}''_{(3)} + \mathbf{v}^{\wedge}_{(3)}. \tag{34}$$

In the configurations considered here, the two types of fluctuations should be distinguished, on first analysis, by appropriate signal processing. Fluctuations of the rotational type $\mathbf{v}''_{(3)}$, essentially associated with turbulence instabilities within the air flow, have the property to be random, while fluctuations of the acoustic type $\mathbf{v}^{\wedge}_{(3)}$, principally associated with the periodic movement due to monochromatic acoustic waves, are periodic. Moreover, as the physical causes, which generate the velocity fluctuations $\mathbf{v}''_{(3)}$ in configuration (3), are the same as those generating $\mathbf{v}'_{(1)}$ in

configuration (1), it is tempting to identify $\mathbf{v}_{(3)}^{\cdot\cdot}$ with the purely random fluctuation velocity $\mathbf{v}'_{(1)}$. In a similar way, it is tempting to identify $\mathbf{v}_{(3)}^{\wedge}$ with the purely periodic acoustic velocity $\mathbf{v}'_{(2)}$.

However, the interaction theory developed by Chu and Kovasznay [20] establishes the fact that velocity fluctuations of different modes may interact and produce new fluctuations of the second order. For this reason, it is probable that random fluctuations propagate relative to the acoustic mode or, conversely, that the acoustic mode generates swirls at a frequency multiple of that of the forced wave. Then, in principle, it is not possible to assert that $\mathbf{v}_{(3)}^{\wedge}$ is purely periodic and $v_{(3)}^{\cdot\cdot}$, purely random.

The previous considerations show that the velocity fluctuations obtained in configuration (3) cannot be modelled without additional experimental data.

3. EXPERIMENTAL STUDY

The theoretical development in section 2 cannot be pursued without additional data relative to the turbulent and acoustic stresses. The present section provides such experimental data. They are relative to low Mach number turbulent air flows in a tube. These air flows are subjected to plane acoustic waves.

3.1. SET-UP AND INSTRUMENTATION

A diagram of the experimental set-up is given in Figure 1. The tube, made from perspex, has an inside diameter of 50 mm and is 5 mm thick. It is made up of several sections, whose length is indicated in the same figure. The sections are assembled using perspex collars with an inside diameter of 60 mm and 60 mm length.

The acoustic waves are generated using a compression chamber with membrane JBL of type 2482. This is placed at one end of the tube. An ending, mounted on the other end, serves to attenuate reflection of the incident waves. This is made up of an exponential horn, the opening of which is obstructed and therefore made airtight by a disk, covered on the side facing the tube with a material which absorbs the intensity of acoustic waves. The length of the tube between the cross-section with the sound emission source and that with the absorbant material of the ending is 7·34 m.

An electrical signal generator sends a sinusoidal signal to the power amplifier which feeds the compression chamber. It is programmed to send out frequencies in the range 300–2000 Hz. The compression chamber is excited with a tension whose value can attain 20 V_{RMS}.

To create suction, a power of approximately 2000 W is available. The air inlet is situated at the absorbant ending side (Figure 1). To ensure that the air inlet disturbs the acoustic wave propagation as little as possible, it is carried out radially on a short section thanks to the apparatus shown in Figure 2. The latter includes triangular sectors to guide the air radially and, close to the tube wall, inclining it with respect to the axis. The suction takes place perpendicularly to the tube axis near the acoustic source.

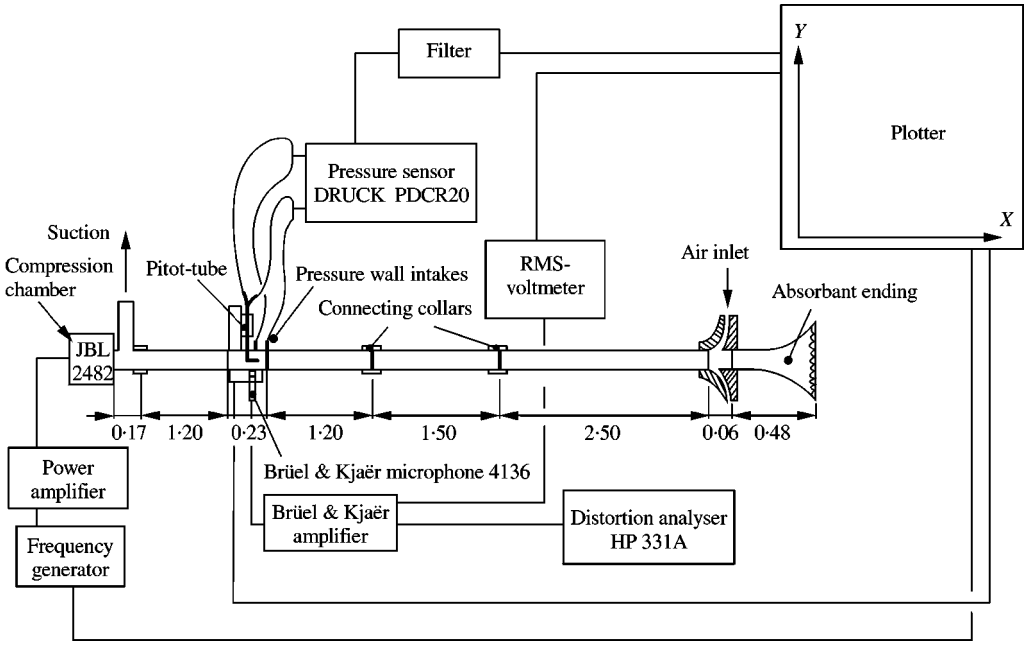

Figure 1. Experimental set-up.

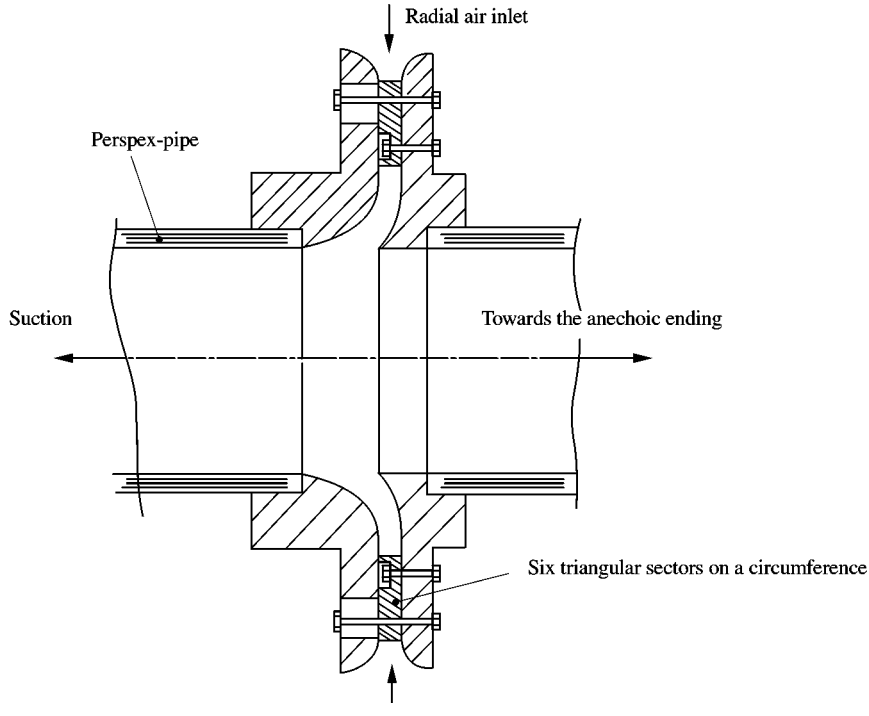

Figure 2. Radial air inlet.

Pressures are measured by means of a Pitot tube with a diameter of 2 mm. The latter is fixed to a sliding translation table following the diameter of the explored cross-section. A pressure differential sensor Druck of type PDCR 20, with a 1·96 mV/mbar sensitivity substracts the static pressure from the total pressure and then converts the difference into an electrical signal. This is then filtered before being recorded. Only the lower frequency components of this signal are retained.

Acoustic pressure is measured using a $\frac{1}{4}$ inch Brüel and Kjäer microphone of type 4136 and the chain of measurement usually associated with this. It is placed in a cylindrical cavity with the same diameter as the microphone and facing inside the tube. For practical reasons, the microphone capsule is set back 15 mm from the inside wall of the tube. The present measurements are not affected, however, by the frequency response of the cavity as the frequency of the first resonance harmonic is 11·33 kHz.

Recording of the electrical signal is analogue and is effectuated using a plotter. The signals are filtered and amplified, if necessary, then recorded according to the vertical position of the Pitot tube or according to the frequency of the waves emitted, relative to the aim of measurement.

3.2. INVESTIGATIONS CARRIED OUT ON THE AIR FLOW WITHIN THE TUBE (CONFIGURATION (1))

The experimental conditions correspond to configuration (1) as defined in section 2.2. The compression chamber is not excited and the air flow is generated using maximum suction power.

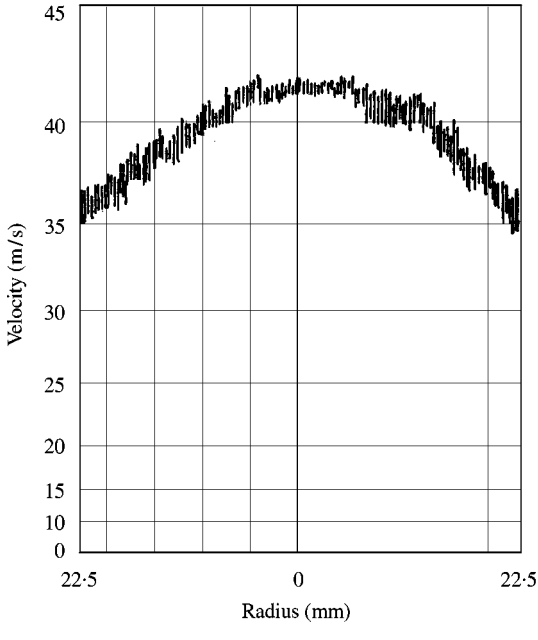

Figure 3. Velocity profile of the air flow without acoustic wave.

The cross-section by which the air enters the tube is located 0·51 m from the absorbent covering of the ending. The measurements relating to the Pitot tube are carried out in a cross-section located 5·41 m from the air-inlet. The suction takes place 1·35 m further downstream.

Flow velocity at the point of measurement is deduced from kinetic pressure measurement. This is obtained from the difference between total pressure and static pressure, simultaneously delivered by the Pitot tube. This difference is provided in the form of an electrical signal by the Druck pressure sensor.

The radial profiles of axial velocities in the cross-section explored are obtained by recording simultaneously the electrical signal and the position of the Pitot tube on the explored diameter. In order to record the mean value of velocity, only low-frequency components of the electrical signal (inferior to 5 Hz) are retained. The translation speed is fixed at 0·25 mm/s.

The radial profile of mean axial velocities thus obtained is shown in Figure 3. It presents a flattened parabolic evolution in the major part of the tube, since the velocity varies by no more than 5 over 90% of the diameter. The amplitude of velocity fluctuations of frequential components inferior to 5 Hz is in the order of 1 m/s. The maximum velocity of 42 m/s, taken at the axis, corresponds to a mean flow velocity of approximately 40 m/s.

3.3. INVESTIGATIONS CARRIED OUT ON THE ACOUSTIC FIELD (CONFIGURATION (2))

The experimental conditions correspond to configuration (2) as defined in section 2.2. The acoustic wave is generated in the medium at rest by exciting the compression chamber.

The tension exciting the compression chamber is sinusoidal. Its frequency is between 300 and 2000 Hz and its value is 13·6 V_{RMS}. Acoustic readings are taken using a microphone, 5·92 m from the side covered with the absorbant material of the absorbant ending, in the cross-section where the radial profile of axial velocities is explored.

The observation, with an oscilloscope, of the signals coming from the microphone shows sine curves more or less distorted according to frequency. Further study of the distortion is undertaken by exciting the compression chamber with a tension of 13·6 V_{RMS}. An HP 331A distorsiometer is used. The study enables the following results to be determined: (1) as the compression chamber emits into free field, the wave distortion rate in the compression chamber is relatively low and concerns 1 to 3% of fundamental; (2) it is notably increased when the compression chamber is in the configuration of emission in the tube, since it attains a mean value in the order of 10% of fundamental at that time. The values, which are in the interval between 7 and 20% of fundamental, are however, closely regrouped around the mean.

Figure 4, which gives the graph for the evolution of RMS-acoustic pressure p_{RMS} according to the frequency, is the result of a frequency range sweep at a velocity of 17 Hz/s. The graph makes apparent regular oscillations of RMS-acoustic pressure according to wave frequency. These oscillations have

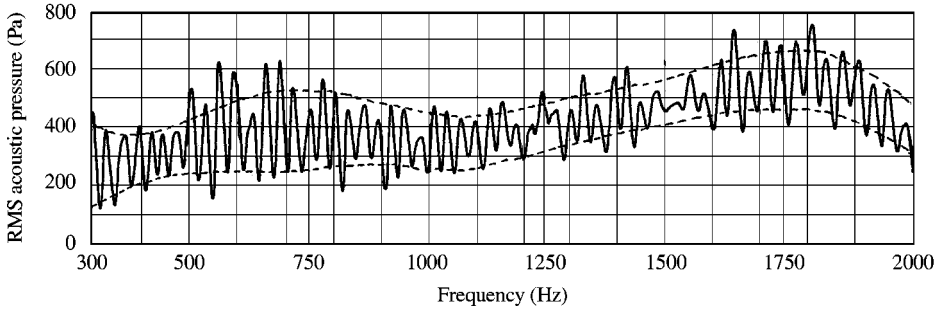

Figure 4. Evolution of the RMS acoustic pressure according to frequency—propagation medium at rest.

a more or less constant period of 29·8 Hz. Inferior and superior envelopes, which delimit the oscillation amplitude, are indicated.

The graph in Figure 4 enables the mean value of the acoustic pressure level present in the tube to be determined. It is in the order of 145 dB (ref. 2×10^{-5} Pa). Readings taken by means of a microphone placed outside the tube, at around 0·05 m from the wall, show that the attenuation produced by the tube wall varies greatly according to the wave frequency and the longitudinal position. The recorded attenuations are evenly distributed throughout the range of 27–52 dB. The mean is in the order of 40 dB.

3.4. INVESTIGATIONS CARRIED OUT ON THE AIR FLOW AND THE WAVE GENERATED SIMULTANEOUSLY (CONFIGURATION (3))

The experimental conditions correspond to configuration (3) as defined in section 2.2. The acoustic wave is generated as described in section 3.3 and the air flow is that described in section 3.2.

The effect of the acoustic wave at a frequency of 400 Hz on the velocity field is evaluated by comparing the reference profile (Figure 3) with that obtained when the wave is emitted into the air flow (Figure 5). The mean of axial velocity is obtained by filtering the electrical pressure signal at 5 Hz, as in the recording shown in Figure 3. The radial profile is obtained by recording simultaneously this signal and the position of the Pitot tube on the explored diameter.

Both the corresponding mean velocity profiles coincide to more than 0·25 m/s. Thus, the acoustic wave modifies only imperceptibly the mean velocity field. Conversely, Figure 5 shows that the acoustic wave has a sizeable influence on the velocity fluctuations, since it reduces the amplitude from a value of 1 m/s to approximately 0·5 m/s.

The effect of the flowing propagating medium on the acoustic field is first evaluated from the evolution of the RMS-acoustic pressure obtained when the wave generated as described in section 3.3 is emitted in the air flow as section 3.1. The graph obtained in this case (Figure 6) is similar to the one obtained when the

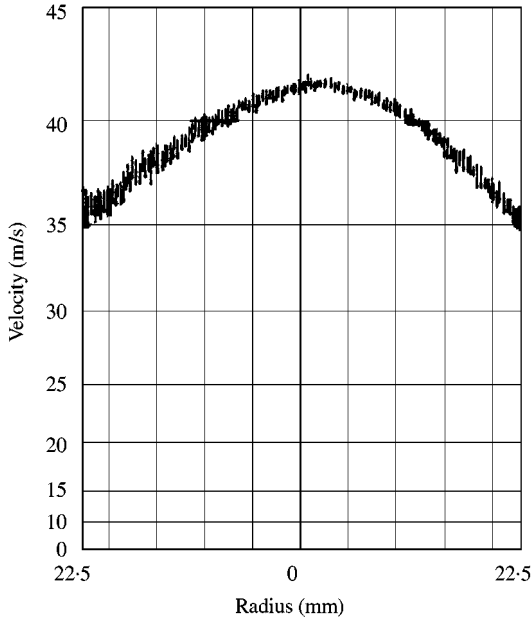

Figure 5. Velocity profile of the air flow subjected to the acoustic wave at 400 Hz.

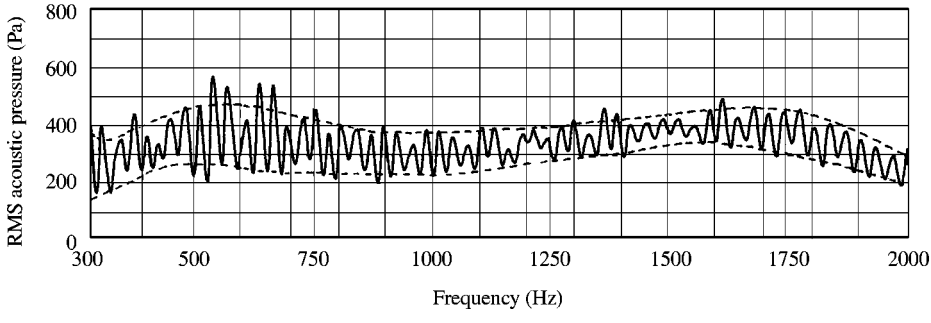

Figure 6. Evolution of the RMS acoustic pressure according to frequency—propagation medium flowing.

air is at rest (Figure 4). The oscillation period, of 29·8 Hz, is equal to that obtained before. The inferior and superior envelopes, which have the same form, are however, closer together, showing a reduction of the oscillation amplitude by a factor of 0·8–0·9, at every wave frequency.

The effect of the flowing propagating medium on the acoustic field is finally evaluated from the study of the rate of distortion. The reading gives values of between 15 and 30% of fundamental and shows an increase in the rate of distortion of between 5 and 10% due to wave propagation in the turbulent air flow. The mean value of the rate of distortion is, however, in the order of 17% of fundamental.

3.5. LONGITUDINAL GRADIENTS OF MEAN PRESSURE NEAR THE INNER WALL

Two pressure intakes 0·14 m apart provide static pressure levels to the wall and allow the measurement of longitudinal gradients of mean pressure produced by the acoustic wave near the inner wall of the tube. The one further upstream, at 5·92 m from the absorbant ending side, is located in the cross-section where the velocity profiles and evolutions of RMS-acoustic pressure according to frequency are recorded.

The difference in the pressures measured in the two cross-sections is given in the form of an electrical signal by the differential pressure sensor. The mean value of this difference is small and requires amplification. An amplification gain of 64 is adopted in the present measurements. This makes it possible to notice that the signal can be distinguished significantly from the background noise of measurement.

Temporal mean is evaluated by the amplitude of the components at the lowest frequencies. The electrical signal is filtered to conserve only the frequential components inferior or equal to 1 Hz. The longitudinal gradient of mean pressure is then evaluated by dividing this amount by the distance which separates the static pressure intakes.

Frequencies in the range 300–2000 Hz are explored at a velocity of 4·2 Hz/s. The procedure for recording the longitudinal gradients of mean pressure consists of superimposing several frequency sweeps. This procedure highlights the reproducibility of the effects measured.

Figure 7 shows two recordings of longitudinal gradients of mean pressure according to wave frequency in the same graph. One is obtained where the acoustic wave is emitted into the medium at rest (configuration (2)) and the other where it is emitted into the permanent turbulent air flow (configuration (3)).

With or without flowing air, the longitudinal gradient of mean pressure shows regular oscillations of a 27·8 Hz period, according to wave frequency. The typical value of oscillation amplitude is obtained at 400 Hz; it is 20 Pa/m. This amplitude can reach 40 Pa/m for other frequencies. In both cases, the envelopes surrounding the oscillation amplitude coincide; they indicate, moreover, that the action of the acoustic wave decreases with the frequency and becomes insignificant from a value to 1000 Hz.

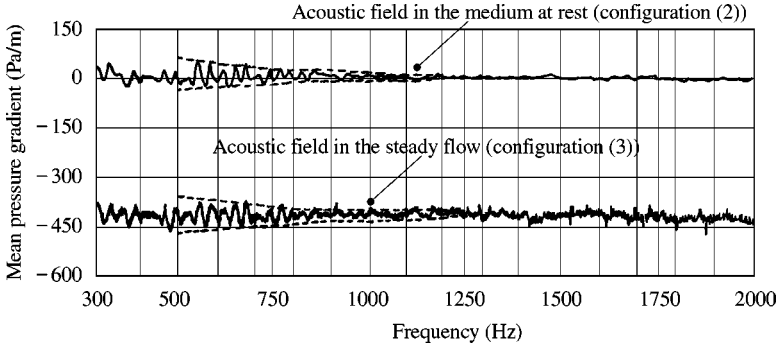

Figure 7. Effect of the frequency on the longitudinal mean pressure gradient.

Finally, the remarkable result here is that, when the wave is emitted into the permanent turbulent air flow, the oscillations are hardly deformed and add to the usual linear loss of pressure. A linear loss of pressure of 450 Pa/m is measured on the readings.

4. VALIDITY OF THE MODELLING

Experimental results analogous to those presented in section 3 are generally described in the framework of the theory of wave instability. However, the formalism issued from that of acoustic streaming (section 2) should be more simple. As its validity has been well established only when propagating mediums are at rest, its validity must be checked in the present case of flowing mediums.

4.1. MODELLING THE AIR FLOW

The hypotheses concerning the modelling of the air flow in the tube (section 2.2) are reviewed and controlled to determine that they have been borne out correctly in the experiments described in section 3.

The mean velocity of air is maximum at the axis and is 42 m/s. The air flow, whose Mach number is greatly inferior to 0·3 (Mach number always inferior or equal to 0·124), can be likened to the flow of an incompressible fluid. Its description by means of Navier–Stokes' equations (1) and (2) is therefore accurate.

The air flow, which takes place within a tube having a diameter of 0·050 m with a mean velocity of 40 m/s, possesses a Reynolds' number of 2 000 000. The value of 2000 defining the upper limit of Reynold's numbers of transition to turbulence being exceeded greatly, the air flow is fully turbulent. Moreover, it is commonly accepted that the permanent regime of flow in tubes is set up for ratios of length to diameter greater than 10, from which point the effects of air-inlet are negligible. As the length of the tube between the inlet and the outlet (6·71 m) is large compared to its diameter (0·050 m), the air flow presents the characteristics of permanent turbulent regime in the greater length of the tube. This makes the modelling of the mean turbulent air flow valid by the statistical equations (3) and (4).

In the absence of device communicating a kinetic moment to the air flow, the latter possesses a purely axial mean movement. Relations (7), (8) and (11) are therefore justified. Moreover, it should be noted that the flattened radial profile of axial velocity (Figure 3) is typical of permanent turbulent regime.

The hypotheses of permanent turbulent flow in incompressible fluid agree with the experimental conditions; in particular, the description by the equations (10), (14) and (16) is relevant.

4.2. MODELLING THE ACOUSTIC FIELD

Each of the hypotheses concerning the modelling of the acoustic field (section 2.3) is first controlled to determine whether it has been borne out correctly in the

experiments described in section 3. The following four hypotheses of Helmholtz' equation (18) are first treated: axisymmetry, linear propagation, monochromatic wave and plane wave.

The axisymmetry of the wave comes from the fact that, in the compression chamber, emission of the acoustic wave is produced by displacing a membrane with axisymmetry following the axis of a tube with axisymmetry. A wave thus generated cannot contain azimuthal structures.

The linearity of wave propagation and the monochromatic wave hypotheses are studied using the measurement of rates of distortion (section 3.3). The high value: 13·6 V_{RMS}, of excitation tension in the compression chamber produces non-negligible rates of distortion which are closely grouped around the mean 10% of fundamental. These rates of distortion which explain all the potential causes of distortion namely: coupling of the acoustic vibrations with the vibrations of the tube wall, distortion at emission by the source, non-linearity of propagation, do not exceed the value of 20% of fundamental. The result is that, irrespective of the wave frequency, at least 75% of the acoustic power is fundamental and, therefore, travels linearly in the form of a monochromatic wave.

It is widely acknowledged that ratios of wavelength to the tube diameter for which the wave is still plane have a maximum value between 3 and 4. The frequencies, which are tested in the range 300–2000 Hz, correspond to a maximum ratio of wavelength to tube diameter of 3·43. The hypothesis of plane wave is here verified.

The calculation hypothesis contained in equation (24) is now dealt with. An overevaluation of $k_T r$ by $|k_T a|$, where a is the tube radius, is carried out using measurements of the attenuation of acoustic intensity by the tube wall. With the smallest attenuation of 27 dB measured at the tube wall (section 3.3), one can write:

$$\frac{I_r}{I_z} = \frac{1}{500}. \tag{35}$$

The radial component of the acoustic intensity I_r is absorbed or transmitted by the wall. The longitudinal one I_z is transmitted following the tube axis. Ignoring the acoustic intensity absorbed into the perspex, and in expressing, at radius a, the components $I_r = \frac{1}{2}\,\mathrm{Re}(p'_{(2)} v'^{*}_{(2),r})$ and $I_z = \frac{1}{2}\,\mathrm{Re}(p'_{(2)} v'^{*}_{(2),z})$ of acoustic intensity by means of formulas (26) and (30), it can be deduced, by approximating $k_T a$ by its modulus $|k_T a|$ that $I_r \propto a|k_T^2|/|k|$ and $I_z \propto 1/|k|$. By noting that the means of $|F(z)|$ and $|H(z)|$ are equal, one gets

$$\frac{I_r}{I_z} \approx \frac{|k_T^2|a^2}{|k|a} = \frac{|k_T^2 a^2|}{|k|a} \approx \frac{1}{500}. \tag{36}$$

In acknowledging that $|k| \approx K \approx \omega/c$, one obtains:

$$|k_T^2 a^2| = \frac{I_r}{I_z}\frac{\omega}{c}a, \tag{37}$$

then the overevaluation valid for all the frequencies less than 2000 Hz:

$$|k_T a| \leqslant 0{\cdot}019. \tag{38}$$

The latter shows that hypothesis $k_T r$ small compared with 1 is verified in the present experiments.

Validity of the modelling is now discussed by comparing the predictions from formula (28) with the experimental results shown in Figure 4. Relation (38) enables the assumption $k_r \approx |k| \approx K \approx \omega/c$ to be made. Application of this approximation in formulas (28) and (29) leads to the prediction of a doubly periodic evolution of RMS-acoustic pressure, according to pulsation ω to be predicted, due to the terms $\cos[2k_r(L-z)-\varphi]$ and $\cos[2k_r L-\varphi]$ present, respectively, in the numerator and denominator of $|F(z)|^2$ (formula (29)).

The periods of oscillation of RMS-acoustic pressure $\Delta f_N = \Delta\omega_N/2\pi$ and $\Delta f_D = \Delta\omega_D/2\pi$, due respectively to the terms $\cos[2k_r(L-z)-\varphi]$ and $\cos[2k_r L-\varphi]$, are calculated by identifying $2(L-z)/c$ with $2\pi/\Delta\omega_N$ and $2L/c$ with $2\pi/\Delta\omega_D$; from the data mentioned in Figure 1 $\Delta f_N = 29{\cdot}3$ Hz and $\Delta f_D = 23{\cdot}4$ Hz are obtained. As these values are close, the oscillations in $p'_{(2)RMS}$ should appear with a beating.

Finally, mathematical study of relation (28) shows that $p'_{(2)RMS}$ does not depend on ω while acoustical properties (reflection coefficient G and specific impedance of the lateral inner wall Z_T) are supposed to be independent of wave frequency.

Readings in Figure 4 confirm all these predictions. Measurement of the period of oscillation from the readings gives the value 29·8 Hz, close to the 29·3 Hz predicted, showing that the period of the numerator of $|F(z)|^2$ (formula (29)) is more important than that of denominator. However, the irregularity of the oscillations, particularly marked in the range 1000–1500 Hz, is easily interpreted as a beating due to interferences with oscillations of close period; this indicates that oscillations due to the denominator of $|F(z)|^2$ cannot be neglected. The lack of any significative tendency, in the tested range of frequencies, concerning the evolution of the oscillation amplitude of $p'_{(2)RMS}$ according to frequencies f, indicates that acoustic properties of the walls, G and Z_T, are not dependent on f; this fact is widely acknowledged for hard materials as perspex in the tested range of frequencies.

The theoretical modelling adopted for the acoustic wave is in satisfactory agreement with the experiment. Formulas (28) and (30) are then, relevant.

4.3. MODELLING THE ACOUSTIC STRESS IN MEDIUM AT REST

The longitudinal gradient of mean pressure experimentally outlined in section 3.5 is obviously an effect of the forced acoustic wave. Here, it is examined as to whether this is a consequence of the acoustic streaming as described by formulas (14) and (32).

First, it should be observed that, in the present experiments, an acoustic streaming undoubtedly exists. Indeed, relation (36) shows that the well-known critical condition for acoustic streaming, which is that of an attenuated wave

[4–6], is realized here. Moreover, the validity of the acoustic wave modelling adopted, highlighted in section 4.2, ensures *a priori* that of formulas (32) giving the acoustic stress $\bar{\tau}_{(2)}$. Finally, the present experimental verification aims to rule out the possibility, in principle, that the longitudinal gradient of mean pressure observed in the air at rest has an origin other than acoustic streaming.

Now, the conditions for which the ratio $\Delta\bar{p}/s$ is representative of the longitudinal gradient of mean pressure $\partial_z\bar{p}$, are determined. Since the value of difference in static pressures $\Delta\bar{p}$ decreases when the distance s separating the measurement cross-sections decreases, it must retain a value sufficiently great for $\Delta\bar{p}$ to be distinguished from the background noise of measurement. The question is to know whether the chosen distance s is sufficiently small.

Configuration (2) of the present experimentations is similar to that of the standard calculation presented by Lighthill in references [6] or [7]. In this configuration, acoustic streaming organizes itself in a periodic spatial structure, where the spatial period is equal to a quarter of the wavelength λ of the wave which generates the acoustic streaming.

The quantity $\Delta\bar{p}/s$ is obviously far from $\partial_z\bar{p}$ when $s \geqslant \lambda/4$. The rough criterion $s < \lambda/4$ arises. With the adopted value $s = 0{\cdot}14$ m, the gradients it is not invalid to approach by $\Delta\bar{p}/s$ must be generated by waves with a frequency f verifying:

$$f \leqslant 605 \text{ Hz}. \tag{39}$$

According to equations (14), the adopted method of measurement, which may provide a representative approximation of $\rho^{-1}\partial_z\bar{p}_{(2)}$, does not allow one to immediately obtain $\bar{\tau}_{(2)}$. However, Lighthill [6] or [7] stresses that, in the standard study of acoustic streaming, Rayleigh [2] then Nyborg [4] and Westervelt [5] make, from the assumption of small acoustic streaming velocities, the hypothesis of negligible convective accelerations and velocity Laplacians. This leads to the identification of the mean pressure gradient to acoustic stress. The present case is no different from the standard one. It is therefore valid to identify $\bar{\tau}_{(2)}$ with $\rho^{-1}\,\mathbf{\nabla}\bar{p}$, and in particular, $\bar{\tau}_{(2)z}$ with $\rho^{-1}\partial_z\bar{p}_{(2)}$.

The verification that the longitudinal gradient of mean pressure generated is due to acoustic streaming is now dealt with. It is based on the equation of system (32) giving $\bar{\tau}_{(2)z}$.

As acoustic properties of the walls do not depend overall on frequencies (section 4.2), the mathematical study of this equation is realized by assuming that G and Z_T are independent of frequency. This study shows that $\bar{\tau}_{(2)z}$ is a periodical function according to f, whose periods are *a priori* those of the terms $p'^2_{(2)RMS}$, $|H(z)|/|F(z)|$ and $\sin(\varphi_H - \varphi_F - \varphi_z)$. It is possible to prove that the periods are, at a good approximation: Δf_N and Δf_N, i.e., those of $p'_{(2)RMS}$ indicated in section 4.2.

The oscillations of $p'_{(2)RMS}$ according to frequency (Figure 4) have an easily detectable period of 29·8 Hz (section 3.3) and another one evaluated at 23·4 Hz, appearing only in a beating (section 4.2). The oscillations of $\Delta\bar{p}/s$ (Figure 7) show a main period of 27·8 Hz (section 3.5), close to the main period of $p'_{(2)RMS}$. Moreover, the attenuation of amplitude observed in the range of frequencies between 400 and 500 Hz could be interpreted as a beating due to interference of the

oscillations at 27·8 Hz with oscillations of close period. The very likely existence of a second period for the oscillations of $\Delta\bar{p}/s$ and the good agreement of the main periods of $p'_{(2)RMS}$ and $\Delta\bar{p}/s$ make it highly probable that the longitudinal gradient of mean pressure is generated according to the modelling proposed in formulas (32).

The same mathematical analysis also shows that the amplitude of the oscillations in $\bar{\tau}_{(2)z}$ increases according to frequency while G and Z_T do not depend on frequency. Now, the reading in Figure 7, relative to the medium at rest, provides a notably different evolution: $\bar{\tau}_{(2)z}$ has a significant value in the range 300–1000 Hz, but the amplitude of the oscillations does not evolve in a well-determined sense according to frequency. Moreover, for frequencies superior to 1000 Hz, the amplitude of $\bar{\tau}_{(2)z}$ is strongly attenuated and disappears in the background noise of measurement.

The validity of the acoustic wave modelling being established up to 2000 Hz (section 4.2), the attenuation from 1000 Hz cannot be due to the fact that one of the hypotheses of this modelling (for example, of the plane wave) should no longer be verified for the present experiments.

Moreover, if the attenuation was due to molecular relaxation, it would occur in a similar way for the RMS-acoustic pressure. The reading in Figure 4 does not show any attenuation in $p'_{(2)RMS}$ up to 2000 Hz. The hypothesis of attenuation due to molecular relaxation does not hold.

On the other hand, it appears that the decrease of oscillation amplitudes begins almost from frequencies for which criterion (39) is no longer valid. It seems that the differences between the predictions concerning the amplitude of the oscillations of $\bar{\tau}_{(2)z}$ and the readings must be attributed to the measurement instrument of pressure gradients. The latter takes pressure at two fixed points in the tube wall. Acoustic streaming being attached to the standing wave, and its wavelength and position varying with the frequency of the wave, the instrument cannot reveal any tendency, according to the only parameter frequency.

In spite of the poor agreement between the predicted and measured evolutions of the amplitude of $\bar{\tau}_{(2)z}$, likely due to the instrument, the good agreement between the oscillation periods of $\bar{\tau}_{(2)z}$ and $p'_{(2)RMS}$ show that formulas (32) are relevant.

5. INTERPRETATION OF THE EXPERIMENTAL RESULTS

The validity of the theoretical modelling in section 2 (section 4) and the more significative experimental data provided in section 3 allows one to pursue now the theoretical development. It results in an interpretation of these data in terms of the influence of air flow on acoustic streaming.

5.1. MOTIVATION AND BASIS OF THE DISCUSSION

It is shown in section 4 that formulas proposed in section 2 for the theoretical modelling of permanent turbulent air flow submitted to acoustic waves generating acoustic streaming, agree with the experiments presented in section 3. However, it is emphasized in section 2.4 that, with no additional information previously available,

this modelling must have left the issue of eventual relations between quantities relative to the three configurations in abeyance.

This issue is in connection with the influence that permanent turbulent air flow may exert on acoustic streaming. The relation

$$\bar{\tau}_{(3)} = \bar{\tau}_{(1)} + \bar{\tau}_{(2)}, \tag{40}$$

seems, intuitively, to be a consequence of additivity of longitudinal mean pressure gradients, experimentally established in section 3.5. It expresses that the stress $\bar{\tau}_{(2)}$ producing acoustic streaming superimposes onto the stress $\bar{\tau}_{(1)}$ inside the permanent turbulent air flow. It is clear that if relation (40) were verified, permanent turbulent air flow would be found to have no influence on acoustic streaming.

The purpose of the present discussion is to establish relation (40) (sections 5.2 and 5.3) and that the high probability for permanent turbulent air flow has no influence on acoustic streaming (section 5.4). Let us note that only a direct measurement of each Reynolds stress in equation (40) would enable the solution of this issue. But, if it is standard to carry out the measurement of purely turbulent stress $\bar{\tau}_{(1)}$ and Reynolds stress $\bar{\tau}_{(3)}$ using a hot-wire, it is on the contrary, difficult to obtain that of acoustic stress $\bar{\tau}_{(2)}$, due to the fact that the fluctuations occur in a medium at rest (see for instance Bruun [21]).

The first experimental result taken as a basis for the present discussion is presented in the last paragraph of section 3.5. It asserts that the longitudinal gradient of mean pressure in configuration (3) is the sum of that produced by the loss of pressure in configuration (1) and of that generated by the acoustic wave in the medium at rest in configuration (2). Taking into account measurement precision, one can write

$$\partial_z \bar{p}_{(3)} \approx \partial_z \bar{p}_{(1)} + \partial_z \bar{p}_{(2)}. \tag{41}$$

The second experimental result is that the profile of mean axial velocities of the turbulent air flow subjected to an acoustic wave at 400 Hz, whose effect on the gradient of mean pressure is significant (section 3.5), is not greatly modified by the acoustic field (section 3.4)

$$\bar{v}_{(3)z} \approx \bar{v}_{(1)z}. \tag{42}$$

The validity of this result, controlled at other frequencies, is assumed for all frequencies.

The third experimental result retained concerns the velocity fluctuations in the different configurations. Some experiments reported in section 3.4 show that the acoustic wave modelling developed in section 2.3 is still valid when the waves propagate in permanent turbulent air flows: readings in Figures 4 and 6 show that oscillation periods in RMS-acoustic pressure and the general shape of inferior and superior envelopes are unchanged by the permanent turbulent air flow. The oscillation amplitude, which is, however, reduced with a factor β comprised

between 0·8 and 0·9, makes it possible to write

$$\mathbf{v}^{\wedge}_{(3)} \approx \beta \cdot \mathbf{v}'_{(2)}. \tag{43}$$

The symbol $\approx$ is used to translate the fact that, thoroughly, the acoustic mode does not coincide exactly with the purely periodic part of the fluctuations (section 2.4).

5.2. APPLICATION OF THE INTERACTION THEORY

The reduction in amplitude of the RMS-acoustic pressure expressed by relation (43) is a consequence of the well-known phenomenon of attenuation due to diffraction by turbulence whose scale is small compared with the wavelength of the wave [22–24].

The interaction theory of Chu and Kovasznay [20] predicts the existence of an interaction between the acoustic mode and the rotational mode of the turbulent air flow. This theory is based on the hypothesis of fluctuations of small amplitude and weak velocity gradients. Then, in configuration (3) of the discussed experiments, the aforementioned consequences are undoubtedly valid in the main.

The interaction between acoustic and rotational modes may be specified. Gaviglio mentions in the book by Favre *et al.* [25] that the effect of this interaction is generally to produce a fluctuation transfer from the acoustic mode to the rotational one, so that, finally, the rotational mode contains all the stochastic fluctuations and the acoustic mode, all the periodic fluctuations. It is clear that approximation (43) then becomes equality:

$$\mathbf{v}^{\wedge}_{(3)} = \beta \cdot \mathbf{v}'_{(2)}, \tag{44}$$

and that it can be written

$$\mathbf{v}^{\cdot\cdot}_{(3)} = \alpha \cdot \mathbf{v}'_{(1)}. \tag{45}$$

The fluctuation transfer between modes is taken into account by the factor α.

Relations (44) and (45) allow transformation of the superposing relation (34) into

$$\mathbf{v}'_{(3)} = \alpha \cdot \mathbf{v}'_{(1)} + \beta \cdot \mathbf{v}'_{(2)}. \tag{46}$$

In writing out relation (46) in formulas (6) and by gathering fluctuations of the same type, the Reynolds stress acting in configuration (3) writes, due to the general property of bilinearity of $\bar{\tau}$ relative to $\mathbf{v}'$:

$$\bar{\tau}_{(3)} = \alpha^2 \cdot \bar{\tau}_{(1)} + \beta^2 \cdot \bar{\tau}_{(2)} + 2\alpha\beta \cdot \bar{\tau}_{(1,2)}. \tag{47}$$

The squares of the velocity fluctuations relative to configurations (1) and (2) provide, respectively, Reynolds stresses $\bar{\tau}_{(1)}$ and $\bar{\tau}_{(2)}$. The cross-products of velocity

fluctuations are grouped together in the mixed stress $\bar{\tau}_{(1,2)}$. In Appendix A, it is shown that the stochastic independence of the random velocity fluctuations $\mathbf{v}'_{(1)}$ and periodic acoustic velocities $\mathbf{v}'_{(2)}$ leads to nil-value of the mixed stress $\bar{\tau}_{(1,2)}$. Relation (47) then becomes

$$\bar{\tau}_{(3)} = \alpha^2 \cdot \bar{\tau}_{(1)} + \beta^2 \cdot \bar{\tau}_{(2)}. \tag{48}$$

When few fluctuations are transferred from the acoustic mode to the rotational one, $\alpha \approx \beta \approx 1$ and relation (48), which expresses the consequences deduced from the interaction theory, becomes equivalent to equation (40).

5.3. APPLICATION OF THE MAIN EXPERIMENTAL RESULTS OBTAINED

Relation (41) plays a central role. It can be transformed into strict equality

$$\partial_z \bar{p}_{(3)} = \partial_z \bar{p}_{(1)} + \gamma \cdot \partial_z \bar{p}_{(2)}, \tag{49}$$

by introducing a factor γ, which expresses the measurement inaccuracy of the amplitude of the longitudinal gradient of mean pressure measurements in configuration (2).

The verification realized in section 4.1 leads to the adoption of systems (10), (14) and (16) as the starting point for the present proof. In fact, only the projection equations following z are retained here

$$\begin{aligned}
\frac{1}{\rho}\partial_z \bar{p}_{(1)} &= -\bar{\tau}_{(1)z} + \nu\left[\partial^2_{r^2}\bar{v}_{(1)z} + \frac{\partial_r \bar{v}_{(1)z}}{r}\right],\\
\frac{1}{\rho}\partial_z \bar{p}_{(2)} &= -\bar{\tau}_{(2)z} - [\bar{v}_{(2)r}\partial_r \bar{v}_{(2)z} + \bar{v}_{(2)z}\partial_z \bar{v}_{(2)z}] + \nu\left[\partial^2_{r^2}\bar{v}_{(2)z} + \partial^2_{z^2}\bar{v}_{(2)z} + \frac{\partial_r \bar{v}_{(2)z}}{r}\right],\\
\frac{1}{\rho}\partial_z \bar{p}_{(3)} &= -\bar{\tau}_{(3)z} - [\bar{v}_{(3)r}\partial_r \bar{v}_{(3)z} + \bar{v}_{(3)z}\partial_z \bar{v}_{(3)z}] + \nu\left[\partial^2_{r^2}\bar{v}_{(3)z} + \partial^2_{z^2}\bar{v}_{(3)z} + \frac{\partial_r \bar{v}_{(3)z}}{r}\right].
\end{aligned} \tag{50}$$

An obvious linear combination of the three equations allows one to write:

$$\begin{aligned}
\frac{1}{\rho}\{\partial_z \bar{p}_{(3)} - \partial_z \bar{p}_{(1)} - \gamma\partial_z \bar{p}_{(2)}\} &= -\{\bar{\tau}_{(3)z} - \bar{\tau}_{(1)z} - \gamma\bar{\tau}_{(2)z}\}\\
&+ \{-[\bar{v}_{(3)r}\partial_r \bar{v}_{(3)z} + \bar{v}_{(3)z}\partial_z \bar{v}_{(3)z}] + \gamma[\bar{v}_{(2)r}\partial_r \bar{v}_{(2)z} + \bar{v}_{(2)z}\partial_z \bar{v}_{(2)z}]\}\\
&+ \left\{\nu\left[\partial^2_{r^2}(\bar{v}_{(3)z} - \bar{v}_{(1)z} - \gamma\bar{v}_{(2)z}) + \partial^2_{z^2}(\bar{v}_{(3)z} - \bar{v}_{(1)z} - \gamma\bar{v}_{(2)z})\right.\right.\\
&\left.\left. + \frac{\partial_r(\bar{v}_{(3)z} - \bar{v}_{(1)z} - \gamma\bar{v}_{(2)z})}{r}\right]\right\},
\end{aligned} \tag{51}$$

and by taking into account the experimental result contained in relation (49), it is deduced:

$$\{\bar{\tau}_{(3)z} - \bar{\tau}_{(1)z} - \gamma \cdot \bar{\tau}_{(2)z}\} = \{-[\bar{v}_{(3)r}\partial_r \bar{v}_{(3)z} + \bar{v}_{(3)z}\partial_z \bar{v}_{(3)z}] + \gamma \cdot [\bar{v}_{(2)r}\partial_r \bar{v}_{(2)z} + \bar{v}_{(2)z}\partial_z \bar{v}_{(2)z}]\}$$
$$+ \left\{ \nu \left[\partial^2_{r^2}(\bar{v}_{(3)z} - \bar{v}_{(1)z} - \gamma \bar{v}_{(2)z}) + \partial^2_{z^2}(\bar{v}_{(3)z} - \bar{v}_{(1)z} - \gamma \bar{v}_{(2)z}) \right.\right.$$
$$\left.\left. + \frac{\partial_r(\bar{v}_{(3)z} - \bar{v}_{(1)z} - \gamma \bar{v}_{(2)z})}{r} \right] \right\}. \tag{52}$$

The experimental result contained in relation (42) may, at first approximation, be replaced by equality

$$\bar{v}_{(1)z} = \bar{v}_{(3)z}. \tag{53}$$

This is allowed by

$$\bar{v}_{(2)z} = 0. \tag{54}$$

Taking into account relations (53) and (54) in equation (52) leads to

$$\bar{\tau}_{(3)z} = \bar{\tau}_{(1)z} + \gamma \bar{\tau}_{(2)z}. \tag{55}$$

This is the particular case of relation (48) obtained in writing $\alpha = 1$ and $\beta = \sqrt{\gamma}$. It is easily shown that the relation $\beta = \sqrt{\gamma}$ is plausible since it comes from relation (44) and homogeneity of $|\bar{\boldsymbol{\tau}}_{(2)}|$ with $|\bar{\mathbf{v}}_{(2)}|^2/a$. Then, relation (55) shows that the present experiments prove the validity of relation (40), at the first approximation.

It is clear that the present measurements do not allow one to establish without doubt the validity of relation (40) in all more advanced approximations. However, it can be noticed that it is sufficient to write

$$\bar{v}_{(3)z} = \bar{v}_{(1)z} + \gamma \bar{v}_{(2)z} \tag{56}$$

and to use the fact that the air flow in configuration (1) is turbulent and permanent (relations (8) and (9)) for relation (55) still be true at order 1.

Lastly, it appears that, when the propagation lengths are sufficiently small, the attenuation factor γ is close to 1 and the additive relation

$$\bar{\tau}_{(3)z} = \bar{\tau}_{(1)z} + \bar{\tau}_{(2)z} \tag{57}$$

holds.

5.4. INFLUENCE OF PERMANENT TURBULENT AIR FLOWS ON ACOUSTIC STREAMING

Relation (40) is proved in two different ways from the experimental results contained in approximations (41)–(43).

Section 5.2 puts forward considerations from the interaction theory to transform approximation (43) derived from the experiments, into an equality. The delicate

point, which is the calculation of the mixed stress is rendered possible by the interaction theory. Indeed, this enables all the stochastic fluctuations to be grouped together in the rotational mode and all the periodic ones in the acoustic mode. The remainder of the proof consists in usual algebraic handlings. In this way, the result is essentially based on the predictions of the interaction theory [20].

Section 5.3 adopts as a starting point relations (10), (14) and (16) coming from the statistic equations of fluid mechanics, whose validity is controlled in section 4.1. The proof uses approximation (41) as its first mainstay. The second one, say approximation (42), only provides the result via the two approximations (53) then (56).

The proof in section 5.3, which is entirely based on experimental results, seems better founded, but relations (53) and (56) express a hypothesis of convection of acoustic streaming by the propagating medium of the wave. This hypothesis is, however, natural because it already applies to the acoustic velocities of waves.

Relation (40) expresses the superimposing of turbulent and acoustic stresses, respectively, relative to configurations (1) and (2). It then translates the absence of interaction between the permanent turbulent air flow and the acoustic streaming. The convection hypothesis contained in equations (53) and (56) agrees with this interpretation of relation (40). The interpretation deduced from the interaction theory, for which fluctuations are extracted from the acoustic mode but do not affect the remainder, is also acceptable.

Finally, relation (40) could be at fault only if, simultaneously, consequences of the interaction theory and the hypothesis of convection of acoustic streaming by permanent turbulent air flow were at fault. It can be deduced that permanent turbulent air flow has, very likely, no influence on acoustic streaming. This is true in the present experiments and more generally every time the propagating medium at rest in which a wave generates acoustic streaming is put into flow in permanent turbulent regime.

Let us note the importance by the hypothesis of permanence of the flow regime. It is easy to see that the present considerations should no longer be valid without the latter.

6. CONCLUSION

The object of the present study is acoustic streaming generated, in permanent turbulent air flow at low Mach numbers, by acoustic waves of high intensity and obeying the linear propagation equation. Practical interest of the study is that of air flows being driven by acoustic means.

The study shows that statistical equations of fluid mechanics are able to describe permanent turbulent air flow submitted to a wave generating acoustic streaming. It also highlights the utility of distinguishing the notions of turbulent and acoustic stresses, according to whether the fluctuations are of random or periodic nature. Lastly, it predicts on the basis of the interaction theory [20] and the present experiments that, in the usual configurations, the acoustic stress add to the turbulent one.

This last result allows resolution of the issue consisting in predicting the Reynolds stress exerted on an air flow subjected to a wave generating acoustic

streaming, since it is deduced from the knowledge of the stresses in two simple configurations: that where the air flow is generated alone and that where the acoustic field is generated alone. A systematic way of modelling the phenomenon is then suggested.

Finally, the study is an illustration that permanent turbulent air flow has very probably no influence on acoustic streaming, the latter being simply convected by the air flow.

REFERENCES

1. M. Faraday 1831 *Philosophical Transactions of the Royal Society of London* **121**, 299–340. On a peculiar classe of acoustical figures and on certains forms assumed by groups of particles upon vibrating elastic surfaces.
2. Lord Rayleigh 1896 *Theory of Sound*. New York: Dover, second edition, 1945 reissue.
3. O. Reynolds 1883 *Philosophical Transactions of the Royal Society* A **175**, 935. An experimental determination of the circumstances which determine whether the motion of water shall be direct or sinuous, and of the law of resistance in parallel channels.
4. W. L. Nyborg 1953 *Journal of the Acoustical Society of America* **25**, 68–75. Acoustic streaming due to attenuated plane waves.
5. P. J. Westervelt 1953 *Journal of the Acoustical Society of America* **25**, 60–67. The theory of steady rotational flow generated by a sound field.
6. M. J. Lighthill 1978 *Journal of Sound and Vibration* **61**, 391–418. Acoustic streaming.
7. M. J. Lighthill 1980 *Waves in Fluids*. Cambridge: Cambridge University Press, Reissue 1980.
8. K. K. Ahuja, J. Lepikovsky and W. H. Brown 1986 *AIAA Paper* 86-1956. 10*th Aeroacoustics Conference*, *Seattle*. Some unresolved questions on hot-jet mixing control through artificial excitation.
9. R. D. Blevins 1985 *Journal of Fluid Mechanics* **161**, 217–237. The effect of sound on vortex shedding from cylinders.
10. J. A. Davis and W. C. Strahle 1990 *Journal of Sound and Vibration* **136**, 121–139. Acoustic vortical interaction in a complex turbulent flow.
11. J. E. Ffowcs-Williams 1988 *Inter-noise* 88, *Proceedings*, 5–20. Active control of "noisy" systems.
12. M. Lowson 1989 *AIAA Paper* 89-1063. 12*th Aeroacoustics Conference*, *San Antonio*. Acoustic forcing of the three dimensional shear layers.
13. J. Shearin and M. Jones 1989 *AIAA Paper* 89-1069, 12*th Aeroacoustics Conference*, *San Antonio*. Airfoil profile increase due to acoustic excitation.
14. C. K. W. Tam 1978 *Journal of Fluid Mechanics* **89**, 357–371. Excitation of instability waves in a two-dimensional shear layer by sound.
15. G. J. Ranque 1933 *Journal de Physique et le Radium* **4**, 112S–115S. Expériences sur la détente giratoire avec productions simultanées d'un échappement d'air chaud et d'un échappement d'air froid.
16. R. Hilsch 1947 *Revue of Scientific Instruments* **18**, 108–113. The use of the expansion of gases in a centrifugal field as cooling process.
17. M. Kurosaka 1982 *Journal of Fluid Mechanics* **124**, 139–172. Acoustic streaming in swirling flow and the Ranque–Hilsch (vortex-tube) effect.
18. L. Landau and E. Lifchitz 1971 *Physique Théorique*. Tome IV Mécanique des fluides. Editions MIR.
19. L. S. G. Kovasznay 1953 *Journal of the Aeronautical Sciences* **20**, 657. Turbulence in supersonic flow.
20. B. T. Chu and L. S. G. Kovasznay 1958 *Journal of Fluid Mechanics* **3**, 494–514. Non-linear interactions in a viscous heat-conducting compressible gas.

21. H. H. Bruun 1995 *Hot-Wire Anemometry*. Oxford: Oxford University Press.
22. A. Ishimaru 1978 *Wave Propagation and Scattering Random Media*, Vol. 2. New York: Academic Press.
23. J. E. Piercy, T. F. W. Embleton and L. C. Sutherland 1977 *Journal of the Acoustical Society of America* **61**. Review of noise propagation in the atmosphere.
24. V. I. Tatarski 1961 *Wave Propagation in Turbulent Medium*. New York: McGraw-Hill.
25. A. Favre, L. S. G. Kovasznay, R. Dumas, J. Gaviglio and M. Coantic 1977 La Turbulence en Mécanique des Fluides. Paris: Gauthiers-Villars.

APPENDIX A: NIL-PROPERTY OF THE MIXED STRESS

The general method proposed by Tatarski [24] to evaluate the mixed stress $\bar{\boldsymbol{\tau}}_{(12)}$ should consist in the evaluation of a correlation function. A simpler method is here rendered possible because of the fact that velocity fluctuations $\mathbf{v}'_{(1)}$ and $\mathbf{v}'_{(2)}$ are stochastically independent. The nil-property of the mixed stress $\bar{\boldsymbol{\tau}}_{(12)}$ will be shown using the notion of T-period conditioned mean, designed by $\langle . \rangle_T$. Let $G(t)$ be a stochastic function of time t. The T-conditioned mean of $G(t)$ relative to time t is defined by

$$\langle G \rangle_T(t) = \lim_{N \to \infty} \frac{1}{N} \sum_{k=1}^{N} G(t + kT). \tag{A1}$$

If $G(t)$ is T-periodic, the immediate consequence:

$$\langle G \rangle_T(t) = G(t + kT) \tag{A2}$$

holds for all integer k and all t in the interval $[0, T]$. Moreover, the period conditioned mean is in connection with the usual stochastic mean by the relation:

$$\bar{G} = \frac{1}{T} \int_0^T \langle G \rangle_T(t) \, \mathrm{d}t. \tag{A3}$$

The function $G(t)$ is now one of the cross-products $v'_X \partial_Y v'_Z$ which make up the components of the mixed stress $\bar{\boldsymbol{\tau}}_{(12)}$. According to formulas (6) and (31),

$$G(t) = v'_{(1)X} \partial_Y v'_{(2)Z} \tag{A4}$$

or

$$G(t) = v'_{(2)X} \partial_Y v'_{(1)Z}. \tag{A5}$$

Here, period T is that of the acoustic wave of pulsation ω:

$$T = \frac{2\pi}{\omega}. \tag{A6}$$

Velocity fluctuations $\mathbf{v}'_{(1)}$ and $\mathbf{v}'_{(2)}$, which are, respectively, stochastic and periodic, still have time derivatives, respectively, stochastic and periodic. The T-conditioned mean of $v'_{(1)X}\partial_Y v'_{(2)Z}$ writes

$$\langle v'_{(1)X}\partial_Y v'_{(2)Z}\rangle_T(t) = \langle v'_{(1)X}\rangle_T(t)\cdot\partial_Y v'_{(2)Z}(t), \tag{A7}$$

and that of $v'_{(2)X}\partial_Y v'_{(1)Z}$ writes

$$\langle v'_{(2)X}\partial_Y v'_{(1)Z}\rangle_T(t) = v'_{(2)X}(t)\cdot\langle\partial_Y v'_{(1)Z}\rangle_T(t). \tag{A8}$$

But, T-conditioned means of $v'_{(1)X}$ and $\partial_Y v'_{(1)Z}(t)$ are nil because of the stochasticity of $\mathbf{v}'_{(1)}$. Then, the ususal mean leads to zero in both cases

$$\langle v'_{(1)X}\partial_Y v'_{(2)Z}\rangle = \frac{1}{T}\int_0^T \langle v'_{(1)X}\rangle_T(t)\cdot\partial_Y v'_{(2)Z}\,\mathrm{d}t = \frac{1}{T}\int_0^T 0\,\mathrm{d}t = 0 \tag{A9}$$

and

$$\langle v'_{(2)X}\partial_Y v'_{(1)Z}\rangle = \frac{1}{T}\int_0^T v'_{(2)X}(t)\cdot\langle\partial_Y v'_{(1)Z}\rangle_T(t)\,\mathrm{d}t = \frac{1}{T}\int_0^T 0\,\mathrm{d}t = 0. \tag{A10}$$

The mixed stress which is a sum of such terms is nil. The announced result is then proved.